RC24655 (W0809-114) September 29, 2008
Physics

IBM Research Report

Field and Bias Dependence of High-frequency Magnetic Noise in MgO-based Magnetic Tunnel Junctions

Y. Guan, D. W. Abraham, M. C. Gaidis, G. Hu, E. J. O'Sullivan, J. J. Nowak, P. L. Trouilloud, D. C. Worledge, J. Z. Sun
IBM Research Division
Thomas J. Watson Research Center
P.O. Box 218
Yorktown Heights, NY 10598

Research Division
Almaden - Austin - Beijing - Cambridge - Haifa - India - T. J. Watson - Tokyo - Zurich

Field and bias dependence of high-frequency magnetic noise in MgO-based magnetic tunnel junctions

Y. Guan*, D. W. Abraham, M. C. Gaidis, G. Hu, E. J. O'Sullivan,
J. J. Nowak, P. L. Trouilloud, D. C. Worledge, and J. Z. Sun
IBM-MagIC MRAM Alliance, IBM T.J. Watson Research Center,
Yorktown Heights, New York 10598

(Dated: September 9, 2008)

Abstract

We present room-temperature measurements of high-frequency magnetization fluctuation (mag-noise) in MgO-based nanopillar magnetic tunnel junctions (MTJs) biased with a direct current (DC). In the frequency range of 1-13 GHz, double mag-noise peaks are observed for some MTJs while others only show a single mag-noise peak. The in-plane field dependence of the mag-noise peak frequency is consistent with the Kittel formula. For all MTJs measured, the bias-dependent shift of the mag-noise peak frequency has a pronounced asymmetry. In addition, we find non-monotonic variations in peak linewidth as a function of the external in-plane magnetic field and of the DC bias current. These suggest the possible involvement of non-macrospin modes in spin-torque-dependent thermal mag-noise generation.

* E-mail address: yguan@us.ibm.com.

INTRODUCTION

Spin-momentum transfer[1, 2] between a spin-polarized direct current (DC) and a ferromagnetic layer provides a controlled manipulation of magnetic moment in nanoscale magnetic structures. For sensors, magnetization fluctuation noise (mag-noise) in a magnetic tunnel junction (MTJ) has become a major concern[3, 4] as its dimension continues to shrink. High-frequency mag-noise in a DC-biased nanoscale MTJ reflects spin-transfer-induced magnetization dynamics and is thus of growing interest[5–10].

High-frequency mag-noise spectrum is similar to that of a typical ferromagnetic resonance (FMR); however, the mechanisms governing the DC-biased mag-noise differ from those in FMR experiments excited by oscillatory currents. When DC biased below the critical current, the system is driven by thermal noise. The field and bias dependence of the mag-noise peak frequency and linewidth could be useful for the study of spin-torque dynamics in MTJs.

Here, we present room-temperature mag-noise measurements between 1-13 GHz as a function of an external in-plane magnetic field and a DC bias current applied to the MgO-based nanopillar MTJs. Double mag-noise peaks are observed for some MTJs while others only show a single mag-noise peak. For all MTJs measured, the in-plane field dependence of the mag-noise peak frequency is consistent with the Kittel formula. The bias-dependent shift of the mag-noise peak frequency is asymmetric for positive and negative bias. In addition, we find non-monotonic dependencies of the mag-noise peak linewidth on the external magnetic field and the bias current.

EXPERIMENT

The mag-noise measurement setup used here is similar to previous reports[4, 6]. The measurements are performed at room temperature on nanopillar MTJs with an external in-plane magnetic field (up to 4 kOe) applied by an electromagnet. A Hall sensor is used to measure the actual field near the measured MTJ. A 50 Ω bias tee with a bandwidth of 80 kHz-26 GHz (5541A Picosecond Pulse Labs) is used to apply a DC bias current to the MTJ, while outputting the mag-noise signals from the MTJ. The electrical contact is made using wire bonding, where the top (bottom) bonding pad of the MTJ is wire bonded to the center (ground) part of a 50 Ω coplanar waveguide (CPW) transmission line. The mag-

noise signals from the MTJ are directed to a 35 dB low-noise amplifier with a bandwidth of 100 MHz-18 GHz (Miteq AFS-series), and then measured using a spectrum analyzer with a frequency range of 9 kHz-26.5 GHz and an input impedance of 50 Ω (ESA E4407B Agilent Technologies).

The resolution bandwidth of the spectrum analyzer is set to 5 MHz and each spectrum is obtained by averaging over 100 spectral scans. For all the mag-noise spectra shown here, the signals at zero bias are subtracted from those measured at nonzero bias. This removes the background Johnson noise as well as the amplifier noise.

We have measured two different types of MgO-based nanopillar MTJs with the following stack composition (in Å): buffer-layer/PtMn(175)/synthetic-antiferromagnet-pinned-layer/MgO(9.5)/Fe(5)/$Co_{60}Fe_{20}B_{20}$(10)/Ru(100)/capping-layer, labeled **A**, and Ta(50)/Cu(200)/Ta(30)/Cu(200)/PtMn(150)/$Co_{70}Fe_{30}$(25)/Ru(8.5)/$Co_{60}Fe_{20}B_{20}$(30)/MgO(12.5)/$Co_{60}Fe_{20}B_{20}$(25)/Ta(50)/Ru(70), labeled **B**. An Anelva I-4500 RIE tool was used to fully pattern both the free and the pinned layers of A-type MTJs, while an ion mill was used to etch the free layers of B-type MTJs with the pinned layers left extended on the scale of tens of micrometers. For both types of MTJs, the top free magnetic layers were etched to elliptical cross-sections of different sizes with long axes parallel to the exchange bias of the bottom pinned layers. We have measured dozens of MTJs from each type. The main results presented here are from a 97×166 nm^2 A-type MTJ with the resistance-area (RA) product of ∼10 Ω μm^2 and the tunneling magnetoresistance (TMR) ratio of ∼80%, labeled **device A**, and a 50×150 nm^2 B-type MTJ with RA ≈ 20 Ω μm^2 and TMR ≈ 160%, labeled **device B**. The external in-plane magnetic field (H) is always applied along the hard axis of the free layer, and the bias current (I) is defined positive when current flows from the top (free) layer to the bottom (pinned) layer.

RESULTS AND DISCUSSION

Fig. 1(a) and (b) show the tunnel resistance (R) as a function of in-plane magnetic field (H) for devices A (for $I = 5\ \mu$A) and B (for $I = 1\ \mu$A), respectively. For device A, a hysteretic behavior exists in the low-field region between -53 Oe and 27 Oe. For device B, the behavior is similar to that reported in Ref. [11]. The difference is due to a small but uncontrolled

offset field which would not affect mag-noise under our measurement conditions.

Fig. 1(c) shows a mag-noise spectrum of device A for H = 1196 Oe and I = -600 μA, where double peaks are clearly observed. Fig. 1(d) shows a mag-noise spectrum of device B for H = 916 Oe and I = -100 μA, where only a single peak is observed. For all the measured values of H and I, double mag-noise peaks corresponding to two distinct modes are always observed and are well defined for device A, while only a single mag-noise peak is always observed for device B. The single-double peak difference between these two devices is possibly due to their different patterned structures. By fitting those mag-noise spectra with a single or double Lorentzian function, both the peak frequency (f) and the linewidth (Δf) are obtained.

The in-plane field dependence of the mag-noise peak frequency for devices A (for I = -600 μA) and B (for I = -100 μA) are presented in Fig. 2(a) and (b), respectively. For both devices, f shifts to higher frequencies with increasing H. The data are well fitted using the Kittel formula for in-plane hard-axis field, similar to[12]

$$f = \frac{\gamma}{2\pi}\sqrt{(H_{eff} - H_k)(H_{eff} + 4\pi M_{eff})}, \tag{1}$$

where γ is the gyromagnetic ratio, H_k is the in-plane uniaxial anisotropy field, M_{eff} is the effective magnetization, and $H_{eff} = H + H_{coupling} + Dk^2/g\mu_B$. $H_{coupling}$ denotes the effective coupling field between the free layer and the pinned layer, which is a few tens of Oe and can be neglected. D is the exchange stiffness, g is the Landé factor, k is the spin-wave wave vector, and μ_B is the Bohr magneton. In fitting the data, we consider only $k = 0$ modes with H_k and $4\pi M_{eff}$ treated as free parameters. For device A, the best fit gives a $4\pi M_{eff}$ value of 1.4$\pm$0.1 kOe for the first mag-noise peak (low frequency) and 3.0$\pm$0.2 kOe for the second mag-noise peak (high frequency), which indicates that the two mag-noise peaks may correspond to two different modes in the coupled free layer-pinned layer system. For device B, the best fit gives $4\pi M_{eff}$ = 5.1$\pm$0.1 kOe. For both devices, the fitted effective magnetization values are smaller than the corresponding bulk values, similar to previous reports[3, 5], which may imply the presence of some out-of-plane magnetic anisotropy field for the free layer.

Fig. 2(c) plots the current-bias dependence of the mag-noise peak frequency for device A for H = 1196 Oe. For the first mag-noise peak (bottom), f increases with increasing negative bias and exhibits smaller change at positive bias. For the second mag-noise peak

(top), f decreases with increasing positive bias and exhibits smaller change at negative bias. Similar trends in peak frequency shift are observed for device A for all the other measured values of H. A bias-dependent asymmetry in the mag-noise peak frequency shift also exists for device B. As shown in Fig. 2(d) for device B for H = 916 Oe, f increases by ∼80 MHz with the negative bias of -130 μA and decreases by ∼35 MHz with the positive bias of 130 μA. This asymmetry, similar to previous reports[11, 13], does not agree with single-domain calculations based on an in-plane or a perpendicular spin torque[14]. A macrospin Landau-Lifshitz-Gilbert (LLG) model with the in-plane spin torque predicts a linear bias-dependent shift in f that is about two orders smaller than the experimental values. The predicted peak frequency shift due to the perpendicular spin torque is of the same order of magnitude as the experimental values; however, it is parabolic and symmetric against bias.

Fig. 3(a) plots the current-field phase diagram for the peak linewidth of the first mag-noise peak of device A, and Fig. 3(b) plots the current-field phase diagram for the mag-noise peak linewidth of device B. As shown in both phase diagrams, Δf depends both on external in-plane magnetic field and on bias current. First, Δf alternatively increases and decreases with H, similar to a recent report[9]. Several stripes in H, corresponding to local maxima or minima of Δf, are observed in both phase diagrams. Secondly, Δf is not a simple monotonic function of I. Opposite shifts in Δf with I are sometimes observed for different H. Similar trends in the field and current dependencies of the mag-noise peak linewidth have been found for all MTJs measured. These features in the current-field phase diagrams for Δf are not explained by macrospin models, where monotonic dependencies of Δf on both H and I are expected.

CONCLUSION

High-frequency magnetic noise measurements have been performed on two different types of MgO-based nanopillar MTJs biased with a direct current. For all MTJs measured, the in-plane field dependence of the mag-noise peak frequency is in good agreement with the Kittel formula. A bias-dependent asymmetry in the mag-noise peak frequency shift is observed. In addition, the mag-noise peak linewidth shows a non-monotonic dependence on external in-plane magnetic field and on bias current. The results suggest the possible involvement of

non-macrospin modes even in sub-critically DC-biased MTJs.

ACKNOWLEDGEMENTS

The authors wish to thank Neil Smith and Jack C. Sankey for helpful discussions. This work is supported under an MRAM development alliance program between IBM and MagIC.

---

[1] L. Berger, Phys. Rev. B **54**, 9353 (1996).

[2] J. C. Slonczewski, J. Magn. Magn. Mater. **159**, L1 (1996).

[3] V. Synogatch, N. Smith, and J. R. Childress, J. Appl. Phys. **93**, 8570 (2003).

[4] G. C. Han *et al.*, J. Appl. Phys. **100**, 063912 (2006).

[5] S. Petit *et al.*, Phys. Rev. Lett. **98**, 077203 (2007).

[6] A. V. Nazarov *et al.*, J. Appl. Phys. **103**, 07A503 (2008).

[7] J.-V. Kim, V. Tiberkevich, and A. N. Slavin, Phys. Rev. Lett. **100**, 017207 (2008).

[8] J.-V. Kim *et al.*, Phys. Rev. Lett. **100**, 167201 (2008).

[9] D. Houssameddine *et al.*, Appl. Phys. Lett. **93**, 022505 (2008).

[10] A. M. Deac *et al.*, Nature Phys., doi:10.1038/nphys1036 (2008).

[11] J. C. Sankey *et al.*, Nature Phys. **4**, 67 (2008).

[12] C. Kittel, *Introduction to Solid State Physics* (Wiley, New York, 2005).

[13] H. Kubota *et al.*, Nature Phys. **4**, 37 (2008).

[14] I. Theodonis *et al.*, Phys. Rev. Lett. **97**, 237205 (2006).

Figures

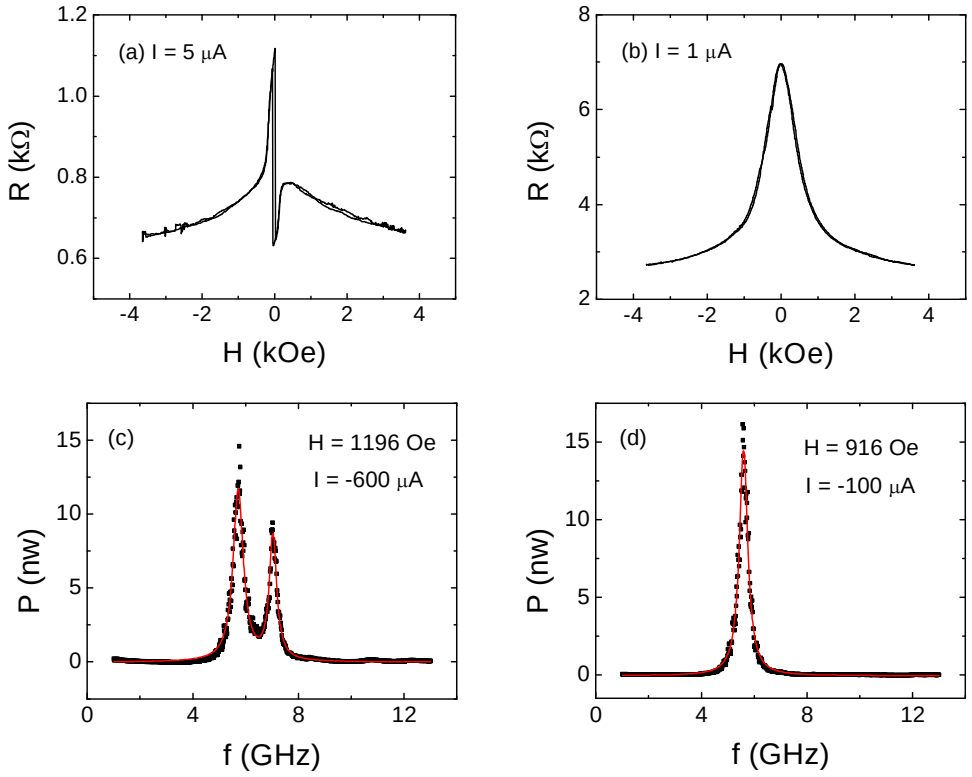

FIG. 1: (Color online) (a) In-plane hard-axis field dependence of the tunnel resistance of device A for $I = 5$ μA; (b) In-plane hard-axis field dependence of the tunnel resistance of device B for $I =$ 1 μA; (c) Mag-noise spectrum of device A for $H = 1196$ Oe and $I =$ -600 μA, including a fit to a double Lorentzian function. (d) Mag-noise spectrum of device B for $H = 916$ Oe and $I =$ -100 μA, including a fit to a single Lorentzian function.

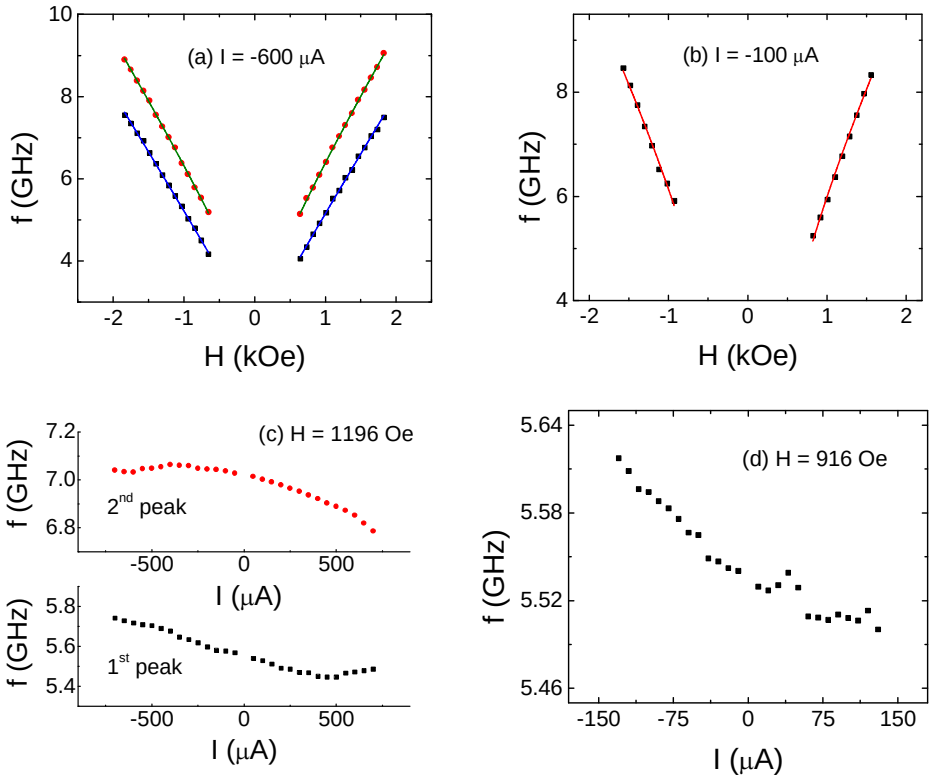

FIG. 2: (Color online) (a) In-plane hard-axis field dependence of the mag-noise peak frequency for device A for I = -600 μA, including fits to Eq. (1); (b) In-plane hard-axis field dependence of the mag-noise peak frequency for device B for I = -100 μA, including fits to Eq. (1); (c) Current-bias dependence of the mag-noise peak frequency for device A for H = 1196 Oe; (d) Current-bias dependence of the mag-noise peak frequency for device B for H = 916 Oe.

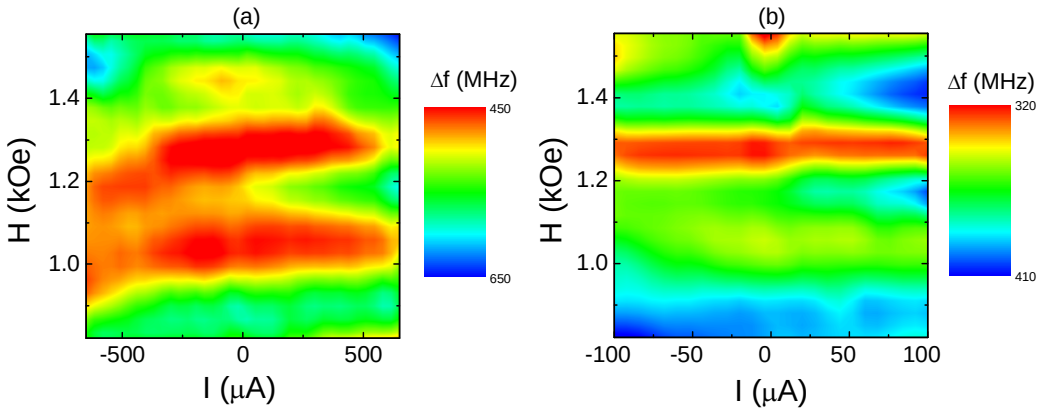

FIG. 3: (Color online) (a) Current-field phase diagram for the peak linewidth of the first mag-noise peak of device A; (b) Current-field phase diagram for the mag-noise peak linewidth of device B.